Performance study of Bayer method red mud based controlled low strength alkali inspired concrete

Abstract

In order to reduce the negative impact of red mud accumulation on the environment, we will recycle red mud to prepare concrete.The controlled low-strength materials were prepared by using red mud, fly ash, and ground granulatedblast furnace slag(GGBS) as raw materials, NaOH as an exciter and polycarboxylic acid water reducing agent as a dispersant, and the working and mechanical properties of the materials were investigated at different ratios of red mud and fly ash. When the mass ratio of red mud to fly ash was 2:1, the dosing of GGBS was 10% and the dosing of NaOH was 1.5%, the maximum flow rate of the mix was 236 mm and the maximum unconfined compressive strength of the specimens at 28 d was 6.5 MPa, which satisfied the specification requirements of controllable low-strength materials. XRD, FTIR and SEM were used to investigate the mineral composition and microstructure of the controllable low-strength material. It was found that the hydration of red mud, fly ash, and GGBS under the action of NaOH formed C-S-H, calcium alumina (AFt), and a small amount of hydrated calcium sulfate, C_4 AF; The strength development of materials is closely related to the flocculent, honeycomb, and lamellar structures of hydration products. The results of this study provide a new technological approach to industrial solid waste scaling in the field of controlled low-strength materials.

Keywords: Compressive, Alkali-activatied cements, Alkali-silica reaction, C-S-H

Introduction

Controlled Low Strength Material (CLSM) is a non-compaction, self-leveling, self-consolidating cementitious material, usually with 28d unconfined compressive strength of less than 8.3 MPa, if CLSM is used as filler for future excavation, the 28d unconfined compressive strength requirement is no more than 2.1 MPa. It is widely used in engineering backfill, pavement base, pipeline bedding and other engineering fields because of its simple preparation process, easy construction and low re-excavation cost[1].It is widely used in the areas of backfilling, pavement bases, pipe bedding, and other engineering applications. Similar to regular concrete, CLSM is mainly composed of cemented materials, aggregates, water and various additives. As the utilization of solid waste resources has been promoted, experts and scholars have conducted numerous studies on the preparation of CLSM from industrial solid waste, which provides an effective way to eliminate industrial solid waste in large quantities [2] .

Red mud is an industrial solid waste discharged from alumina industry, and the current utilization rate is less than 10%.[3] The utilization rate is currently less than 10%. Due to the fine particle size, strong alkalinity and high Na_2 O content of red mud, it is difficult to be used in large quantities in building materials such as silicate cement and concrete. However, the main components of red mud (CaO, SiO_2 , Al_2 O_3 , etc.) are necessary and beneficial for alkali-induced cementitious materials. Therefore, the development of advanced alkali-excited technologies for the preparation of controlled low strength materials using red mud as a raw material and improving the utilization of red mud are of great importance for the application of industrial solid

waste reduction and environmental protection.TAN et al. [4] The results showed that the fluidity of CLSM decreased when the cement substitution rate increased from 0 to 30%, but the water secretion rate was improved and the hydration process was accelerated; the 28d compressive strength of CLSM was best when the cement substitution rate was 15%, and all the indexes of CLSM met the standard requirements under the test substitution rate. [5] used silicate cement as cementitious agent and mixed with industrial solid waste such as red mud, fly ash and phosphogypsum to evaluate the engineering properties of CLSM such as flowability, compressive strength, water secretion rate and durability under different matching ratio conditions, which confirmed the feasibility of red mud in the preparation of cement-based controllable low strength materials.The existing research results show that red mud is feasible as a partial substitute for Portland cement in the production of controllable low-strength materials, but the strength formation mechanism of the study is not in-depth.

In this paper, controlled low strength materials were prepared with red mud and fly ash as the main raw materials, ground granulatedblast furnace slag as auxiliary materials and NaOH as alkali exciter, and their working and mechanical properties were evaluated to investigate the microscopic mechanism of strength development of controlled low strength materials prepared from red mud-based total solid waste, in order to provide a technical reference for the preparation of controlled low strength materials from red mud-based total solid waste.

1. Materials and methods

1.1 Test material

(1) Red mud (RM). The test red mud was taken from an aluminum industrial plant in Henan, which is Bayer method red mud with a density of 3.2g/cm^3 ,d50 of 16. 33μm and a red powder appearance, and its chemical composition and XRD analysis results are shown in Table 1 and Figure 1, respectively.

Table 1 Analysis results of the chemical composition of the red mud. %

Element	SiO_2	Al_2O_3	CaO	Fe_2O_3	Na_2O	TiO_2	K_2O	LOI
Content(%)	10.7	17.5	1.32	55.7	8.15	4.12	0.13	2.38

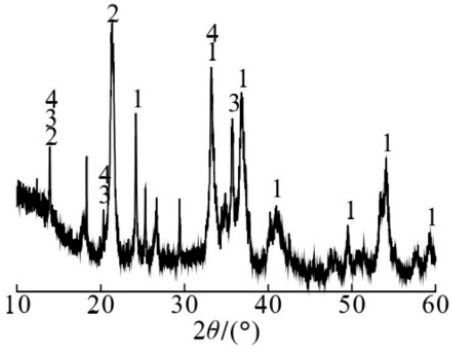

Fig. 1 XRD pattern of the RM.

1-Fe_2O_3 ;2-SiO_2 ; 3-Titanium minerals; 4-$AlNaO_6Si_2$

From Table 1 and Figure 1, it can be seen that the main components of the Bayer RM are Fe_2O_3, Al_2O_3, SiO_2 and also include a small amount of titanium minerals and sodium silica-aluminate hydrate.

(2)Fly ash (FA). The test FA was taken from a power plant in Henan province and is a Class F FA. The chemical composition and XRD analysis results are shown in Table 2 and Figure 2, respectively.

Table 2 Analysis results of the chemical composition of the FA. %

Element	SiO_2	Al_2O_3	CaO	Fe_2O_3	SO_3
Content(%)	45.6	34.6	4.54	10	1.73

Element	Na_2O	TiO_2	K_2O	MgO	LOI
Content(%)	0.16	1.25	0.75	0.67	0.7

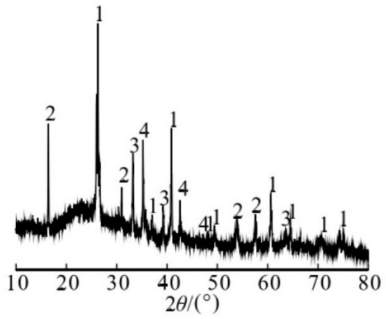

Fig. 2 XRD pattern of the FA.

1-alpha-quartz;2-mullite;3-hematite;4- calcite

As shown in Table 2 and Figure 2, the main components of FA are SiO_2 , Al_2O_3 and Fe_2O_3 ; the main phases are α-quartz, mullite, hematite and calcite.

(3) Ground granulatedblast furnace slag(GGBS). The GGBS was provided by Yongfeng Iron and Steel Co., Ltd. The chemical composition and XRD analysis results are shown in Table 3 and Figure 3, respectively.

Table 3 Analysis results of the chemical composition of the GGBS.%

Element	SiO_2	Al_2O_3	CaO	Fe_2O_3	SO_3
Content(%)	29.75	14.24	41.45	1.7	2.75

Element	Na_2O	MgO	MnO_2	LOI
Content(%)	0.55	7.65	0.53	1.38

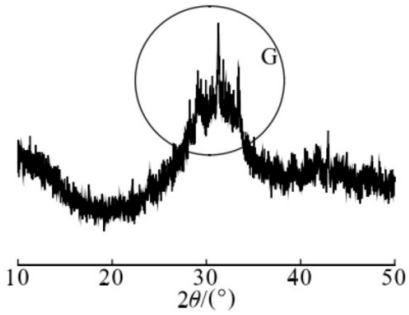

Fig. 3 XRD pattern of the GGBS.

G-Amorphous phase calcium-silica-aluminium minerals

As can be seen from Table 3 and Figure 3, the main components of the GGBS are CaO, SiO_2 and Al_2O_3; The main phase is an amorphous calcium-silica-aluminium mineral.

(4) Alkali exciter and admixture. The alkali exciter used in the test is NaOH with 96%; the admixture is water reducing agent polycarboxylic acid produced by Tianjin Weihe Science and

Technology Development Co.

1.2 Test method

1.2.1 Proportional design and specimen preparation

The controlled low strength material was prepared by fixing the dosing of GGBS at 10%, adjusting the dosing of RM and FA, adding alkali exciter and 0.75% water reducing agent polycarboxylic acid by external doping method, and exploring the effect of NaOH dosing (1%, 1.5% and 2%) on the 28d unconfined compressive strength of the specimens, the specific ratio design is shown in Table 4.

Table 4 Design of test proportion(%)

Samples	RM	FA	GGBS
S1	45	45	10
S2	50	40	10
S3	55	35	10
S4	60	30	10
S5	65	25	10
S6	70	20	10

Weigh the RM, FA and GGBS according to the ratio design in Table 4, and then weigh the polycarboxylic acid water reducing agent of 0.75% of the total mass of the above materials, and mix well. Add NaOH to a certain amount of water and mix it fully until it is completely dissolved. After the NaOH solution is cooled to room temperature, pour the well-mixed material into the NaOH solutionand then place it in NJ-160A mixer for mixing according to the standard. After the mixing is completed, it is poured into a 50.5 mm×50.5 mm×50.5mm mold, and then put into a constant temperature and humidity maintenance box (maintenance temperature is 20±2□, humidity≥50%) for maintenance.

1.2.2 Performance characterization

According to ASTM D6103 cylinder test method, the flow size of the mix was measured by a standard cylinder test mold of ϕ75mm×150mm; The 28d unconfined compressive strength of the cubic specimen was tested according to ASTM D4832, three times for each set of tests, and the average value was taken; The specimens maintained for 28d were crushed and placed in anhydrous ethanol to terminate hydration, and XRD, FTIR and SEM analyses were performed.

2. Results and Discussion

2.1 Effect of RM dosing on 28 d unconfined compressive strength of specimens at different NaOH dosing levels

Figure 4 shows the effect of RM dosing on the 28 d unconfined compressive strength of the specimens at different NaOH doses.

From Fig. 4, it can be seen that: (i)the 28d unconfined compressive strength of the specimen increases and then decreases with the increase of RM dosing under the same NaOH dosing; (ii) the 28d unconfined compressive strength of the specimen increases with the increase of NaOH dosing under the same RM dosing.

The 28-d unconfined compressive strength of the specimens reached the maximum value when the mass ratio of RM to FA was 60:30, and the 28-d unconfined compressive strength of the specimens reached 4.2, 6.5, and 7.2 MPa when NaOH was dosed at 1%, 1.5%, and 2%, respectively, which was mainly due to the reduction of the active silica-alumina raw materials in the system due to the excessive dosing of RM, which was insufficient to stimulate the formation

of an effective polymer structure, resulting in the reduction of the compressive strength. The 28-d lateral compressive strength of the specimens was less than 2.8 MPa when the Na OH dose was 1% and the RM dose was 45% and 50%, which did not meet the requirements of the CLSM specification; when the NaOH dose was 1.5% and 2%, the 28-d lateral compressive strength of the specimens was greater than 2.8 MPa and less than 8.3 MPa when the RM dose was tested, which met the requirements of the CLSM specification. In summary, under the condition of certain amount of GGBS doping, the highest reaction degree and the largest material utilization rate were achieved when the mass ratio of RM to FA was 2:1. In the case that the NaOH dosing of 1.5% and 2% meet the specification requirements, the subsequent test was conducted with the specimen of NaOH dosing of 1.5% as the object of study.

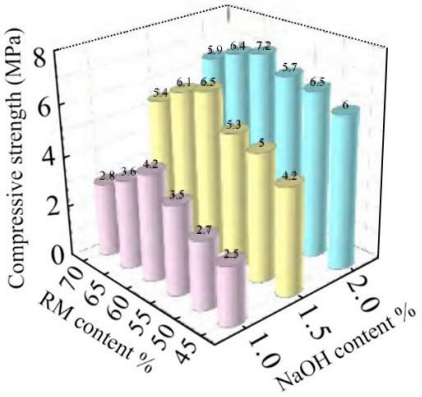

Fig. 4 Influence of the RM addition on 28 d unconfined compressive strength of the samples with different amount of NaOH.

2.2 Effect of water-solid ratio and RM admixture on the flow of CLSM

The effects of water-solid ratio and RM dosing on the CLSM flow rate were investigated under the condition of Na OH dosing of 1. 5%, and the results are shown in Fig. 5.

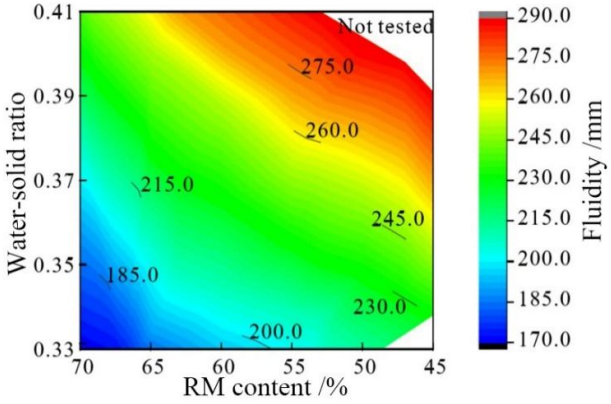

Fig. 5 Influence of water to solid ratio and RM addition on fluidity of CLSM.

From Fig. 5, it can be seen that CLSM with high water-solid ratio and low RM admixture has good flowability and the water requirement increases with the increase of RM admixture. The corresponding water-solid ratios are 0.385, 0.370, and 0.353 when the flow degree is 230 mm and the RM admixture is 70%, 60%, and 50%, respectively. Since the requirement of flow degree for controllable low strength materials is not less than 180 mm[6, 7] the minimum water-solid ratio was chosen to be 0.35 when the RM admixture reached a maximum of 70%.

The effect of RM admixture on the CLSM flow rate under the conditions of 1.5% NaOH admixture and 0.35 water-solid ratio is shown in Figure 6.

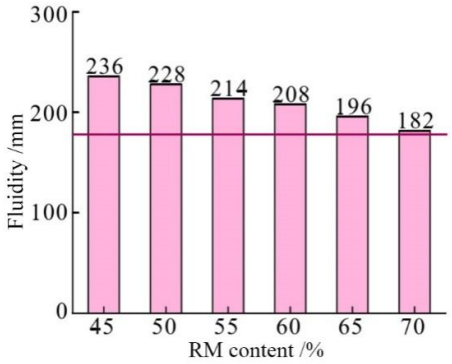

Fig. 6 Influence of RM addition on fluidity of CLSM.

From Fig. 6, it can be seen that the CLSM flowability is negatively correlated with the RM admixture. When the RM admixture is 45%, the flowability reaches 236 mm, while when the RM admixture increases to 70%, the flowability is only 182 mm. Analysis suggests that this is mainly due to the fact that the flowability size of the system is influenced by the specific surface area of RM[8]. The specific surface area of RM is relatively large, and under the condition that the water-solid ratio is determined, the amount of water adsorbed on the surface of RMincreases with the increase of its admixture. In addition, due to the spherical shape of FA, the surface structure is round and dense, which can significantly improve the fluidity of the slurry [9]. However, the fluidity of CLSM decreases significantly as the amount of RMincreases and the amount of FA decreases.

Therefore, for the RM - FA - GGBS system, to meet the flow performance requirements of CLSM, the water-solid ratio of 0.35 is the most economical and reasonable under the condition of constant GGBS admixture, and when the admixture of RM is less than 60%, the medium-high flow degree (200 mm) requirements of CLSM can be achieved.

2. 3 XRD analysis

Figure 7 shows the results of XRD analysis of the specimens after 28 d of curing.

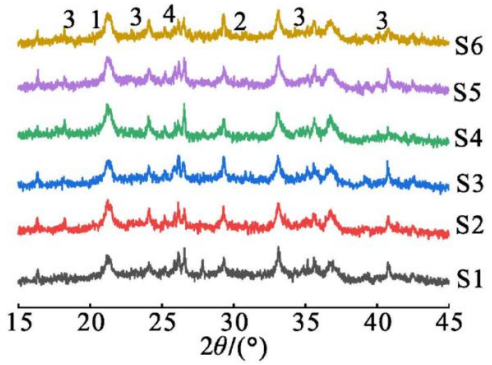

Fig. 7 XRD patterns of the CLSM specimens cured for 28 days.

1-$Ca_6 Fe_2 (SO_4)_3 (OH)_{12} \cdot 26H_2O$; 2-$Ca_5 (SiO_4)_2 CO_3$.

3-AFt; 4-$Na_6 [(Si,Al)_6 O_{24}](Ca_2 CO_3)\cdot(H_2 O)_2$

As can be seen from Fig. 7, the hydration products of CLSM under different matching ratio conditions are basically the same, mainly calcium alumina, silica calcite, calcium chalcocite and

hydrated calcium sulfate ferrate. After the addition of NaOH to the material, the reactive oxides in RMreact with FA and GGBSunder alkaline environment, and the silica-oxygen tetrahedra and alumina-oxygen tetrahedra decompose, and the silica-oxygen and alumina-oxygen bonds break and rebondto form Si-O-Al polymers as well as AFt [10, 11] . The reactive SiO2 in RM dissolves under the excitation of NaOH and reacts with Ca^{2+} and CO2 in the air to finally form silica calcite[11] The hydrated calcium thiosulfate belongs to the AFm phase, and Fe_2O_3 in the RM replaces part of Al_2O_3 in the hydration reaction to produce hydrated calcium thiosulfate. In this system, part of C_3A is hydrolyzed to form AFt [12] which indicates the formation of silica-alumina-oxygen polymer cemented AFt crystals as well as other hydration products in this system. Some of the AFt diffraction peaks in the figure became sharp, while the diffraction peaks of the other hydration products hardly changed with the different ratios, which indicates that no new phases appeared with the change of the raw material ratios.

2. 4 FTIR analysis

Figure 8 shows the results of FTIR analysis after 28 d of specimen maintenance.

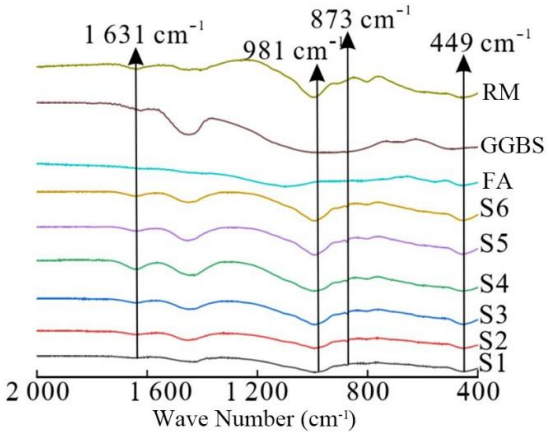

Fig. 8 FTIR patterns of the CLSM specimens cured for 28 days.

In a general sense, 900~1200 cm^{-1} are the characteristic peaks of the main band of alkali-excited gelling materials, where the Si-O-Si stretching vibrations in [SiO_4] at around 1200, 1100, 960, 900 cm^{-1} are C-S-H [13, 14] . The absorption bands at 449 cm^{-1} and 981 cm^{-1} belong to the bending vibration absorption peaks of Si-O-Si (Al, Fe), which are the characteristic bands of tobermorite and C-S-H gels[15]. The bending vibration of H_2O in the C-S-H gel was observed at 1631 cm^{-1}[16]. In addition, the weak absorption peak at 873 cm^{-1} is the result of the solid solution of Fe by the hydration product AFt, and the small substitution of Fe for Al leads to the decrease of the symmetry of AFtand the weak red shift of the band[17].

Combined with the results of XRD analysis, this suggests that some of the reactive Fe_2O_3 in the RM will replace Al_2O_3 in the hydration reaction to form hydrated calcium sulphate ferrate[18]. In addition, the slight shift of the spectral band at 873 cm^{-1} may also be related to the formation of C_4AF. In general, the characteristic peaks of CLSM did not change significantly under different matching conditions, indicating that the mineral composition and content of the hydration products of each specimen were generally consistent.

2.5 SEM analysis

In order to further analyze the morphology, grain size and distribution of hydration products after 28d curing of the specimens under different ratio conditions, SEM analysis was performed

and the results are shown in Fig. 9.

From Fig. 9(a), it can be seen that when the mass ratio of RM to FA is 45∶45, there are more clusters of unreacted RM, and a small amount of AFt is generated at the same time.

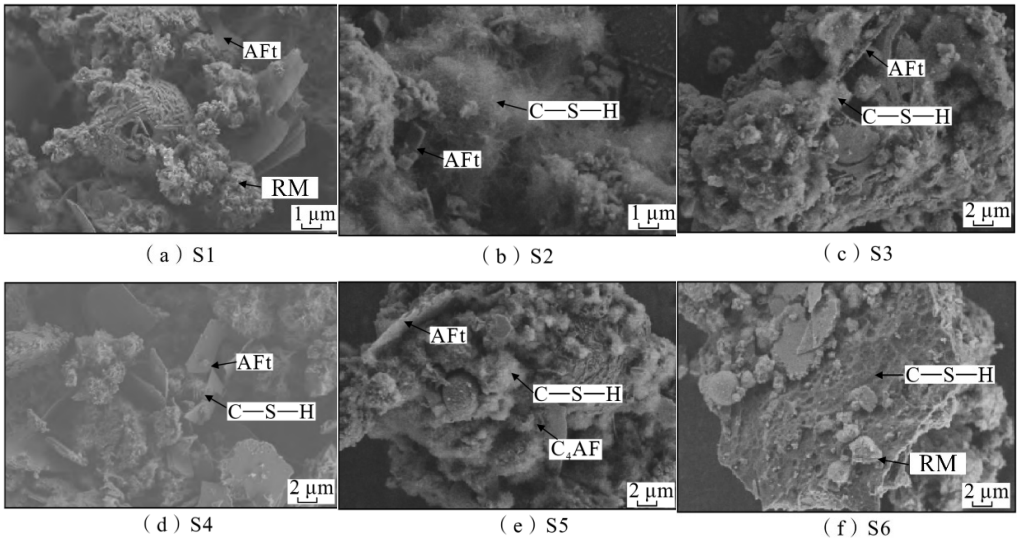

(a) S1 (b) S2 (c) S3

(d) S4 (e) S5 (f) S6

Fig. 9 SEM images of the CLSM specimens cured for 28 days.

From Fig. 9(b), it can be seen that with the increase of RM admixture, the alkalinity of the system gradually increased, and the honeycomb hydration products C-S-H with larger porosity and AFt and some uninvolved FA appeared, and the overall structure was looser, so the strength was also lower.

From Fig. 9(c) and (d), it can be seen that when the mass ratio of RM to FAis 55∶35, denser C-S-H and a small amount of AFt are produced, porosity decreases, and CLSM strength increases; when the mass ratio of RM to FAreaches 60∶30, the hydration products AFt increase, and are densely linked and cross-linked with silica and aluminum-oxygen gel polymers and C-S-H, as well as with other crystals The hydration products fill and lap each other to form a composite double structure with strength[18-20].

From Fig. 9(e) and (f), it can be seen that when the red mud admixture is further increased, the calcium alumina decreases and the CLSM strength decreases; when the amount of RM admixture is too much, the hydration products are relatively reduced with the reduction of active silica-alumina substances in the system and cannot provide sufficient strength for the structure, which echoes the trend of the compressive strength results.

In addition, the prismatic product of the white intermediate phase can be seen in Figure 9(e) (Figure 10), presumably as C_4 AF[21] . It was found that the strength of the iron phase slurry is mainly dependent on the colloidal-crystalline cementation structure; in high alkalinity slurries, the iron phase is less gelatinous [22] This explains the shift of the spectral band at 873 cm^{-1} and the decrease in intensity due to the solid solution of Fe by AFt in FTIR.

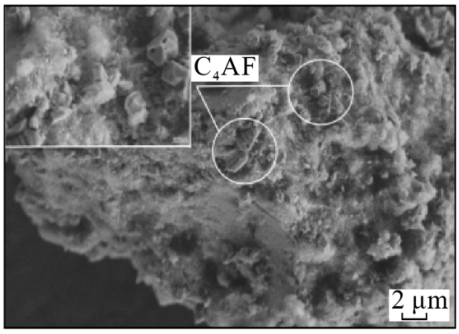

Fig. 10 Micromorphology of C_4 AF in CLSM system.

3. Conclusion

(1) With the increase of RM dosing, the 28d unconfined compressive strength of the specimens first increased and then decreased, and the compressive strength of the specimens reached the maximum when the mass ratio of RM to FA was 60∶30. In addition, the size of the flow rate is affected by both the specific surface area of RM and the amount of FA admixture, and the flow rate decreases when the amount of RM admixture increases and the amount of FA admixture decreases; when the mass ratio of RM to FA is 70∶20, the flow rate is within the defined permissible range, and the flow rate is 182 mm.

(2) NaOH as an exciter can activate the system of RM, FAand GGBS, and the 28d unconfined compressive strength of the specimens can reach 4.2~6.5 MPa and the flow degree is 182~236 mm when the NaOH dosing is 1.5%.

(3) The hydration products of the NaOH-excited system mainly include C-S-H gel polymer and AFt; in addition, in AFt Fe_2O_3 will replace part of Al_2O_3 to participate in the hydration reaction to produce hydrated calcium sulfate and iron, and part of Fe^{3+} in the RM replaces Al^{3+} to possibly produce C_4 AF. The gel and crystals in the microstructure are filled with each other and cross bonded to form a relatively dense structure, which provides a microstructural support for the formation of a certain strength of CLSM. CLSM provides microstructural support.

Reference.

[1] C. Wang, Y. Li, P. Wen, W. Zeng, X. Wang, A comprehensive review on mechanical properties of green controlled low strength materials, Construction and Building Materials, 363 (2023) 129611.

[2] M. Ibrahim, M.K. Rahman, S.K. Najamuddin, Z.S. Alhelal, C.E. Acero, A review on utilization of industrial by-products in the production of controlled low strength materials and factors influencing the properties, Construction and Building Materials, 325 (2022) 126704.

[3] B. Bai, F. Bai, X. Li, Q. Nie, X. Jia, H. Wu, The remediation efficiency of heavy metal pollutants in water by industrial red mud particle waste, Environmental Technology & Innovation, 28 (2022) 102944.

[4] T.M. Do, Y.-s. Kim, Engineering properties of controlled low strength material (CLSM) incorporating red mud, International Journal of Geo-Engineering, 7 (1) (2016) 7.

[5] V.K. Singh, S.K. Das, Engineering Properties of Industrial By-Product-Based Controlled Low-Strength Material, in: M. Latha Gali, P. Raghuveer Rao (Eds.) Problematic Soils and Geoenvironmental Concerns, Springer Singapore, Singapore, 2021, pp. 277-294.

[6] Y.-s. Kim, T.M. Do, H.-k. Kim, G. Kang, Utilization of excavated soil in coal ash-based controlled low strength material (CLSM), Construction and Building Materials, 124 (2016) 598-605.

[7] T. Manh Do, G.-O. Kang, Y.-s. Kim, Development of a new cementless binder for controlled low strength material (CLSM) using entirely by-products, Construction and Building Materials, 206 (2019) 576-589.
[8] L. Santona, P. Castaldi, P. Melis, Evaluation of the interaction mechanisms between red muds and heavy metals, Journal of Hazardous Materials, 136 (2) (2006) 324-329.
[9] S.M.A. Qaidi, B.A. Tayeh, H.U. Ahmed, W. Emad, A review of the sustainable utilisation of red mud and fly ash for the production of geopolymer composites, Construction and Building Materials, 350 (2022) 128892.
[10] H. Quan, H. Yu, D. Lv, Y. Li, The Use of Slag and Red Mud for the Synthesis of a Slag-Based Cementitious Material, Journal of Physics: Conference Series, 2329 (1) (2022) 012036.
[11] K. Tian, Y. Wang, S. Hong, J. Zhang, D. Hou, B. Dong, F. Xing, Alkali-activated artificial aggregates fabricated by red mud and fly ash: Performance and microstructure, Construction and Building Materials, 281 (2021) 122552.
[12] P.K. Mehta, Mechanism of expansion associated with ettringite formation, Cement and Concrete Research, 3 (1) (1973) 1-6.
[13] H. Xu, J.S.J. Van Deventer, Geopolymerisation of multiple minerals, Minerals Engineering, 15 (12) (2002) 1131-1139.
[14] I. Ozer, S. Soyer-Uzun, Relations between the structural characteristics and compressive strength in metakaolin based geopolymers with different molar Si/Al ratios, Ceramics International, 41 (8) (2015) 10192-10198.
[15] H. Ma, H. Zhu, C. Wu, H. Chen, J. Sun, J. Liu, Study on compressive strength and durability of alkali-activated coal gangue-slag concrete and its mechanism, Powder Technology, 368 (2020) 112-124.
[16] Z. Li, J. Zhang, S. Li, C. Lin, Y. Gao, C. Liu, Feasibility of preparing red mud-based cementitious materials: Synergistic utilization of industrial solid waste, waste heat, and tail gas, Journal of Cleaner Production, 285 (2021) 124896.
[17] J.P. Rebouças, J.J.R. Rohwedder, C. Pasquini, Near infrared emission spectroscopy for rapid compositional analysis of Portland cements, Analytica Chimica Acta, 1024 (2018) 136-144.
[18] T. Lan, Y. Meng, T. Ju, M. Song, Z. Chen, P. Shen, Y. Du, Y. Deng, S. Han, J. Jiang, Manufacture of alkali-activated and geopolymer hybrid binder (AGHB) by municipal waste incineration fly ash incorporating aluminosilicate supplementary cementitious materials (ASCM), Chemosphere, 303 (2022) 134978.
[19] T. Hertel, Y. Pontikes, Geopolymers, inorganic polymers, alkali-activated materials and hybrid binders from bauxite residue (red mud) - Putting things in perspective, Journal of Cleaner Production, 258 (2020) 120610.
[20] X. Cheng, D. Long, C. Zhang, X. Gao, Y. Yu, K. Mei, C. Zhang, X. Guo, Z. Chen, Utilization of red mud, slag and waste drilling fluid for the synthesis of slag-red mud cementitious material, Journal of Cleaner Production, 238 (2019) 117902.
[21] W. Wang, X. Wang, J. Zhu, P. Wang, C. Ma, Experimental Investigation and Modeling of Sulfoaluminate Cement Preparation Using Desulfurization Gypsum and Red Mud, Industrial & Engineering Chemistry Research, 52 (3) (2013) 1261-1266.
[22] B.J. Zhan, D.X. Xuan, C.S. Poon, C.J. Shi, Mechanism for rapid hardening of cement pastes under coupled CO2-water curing regime, Cement and Concrete Composites, 97 (2019) 78-88.